Current Biology *16*, 636–648, April 4, 2006 ©2006 Elsevier Ltd All rights reserved DOI 10.1016/j.cub.2006.02.067

Article

nsf Is Essential for Organization of Myelinated Axons in Zebrafish

Ian G. Woods,[1] David A. Lyons,[1] Matthew G. Voas,[1] Hans-Martin Pogoda,[1] and William S. Talbot[1,*]
[1] Department of Developmental Biology
Stanford University
Stanford, California 94305

Summary

Background: Myelinated axons are essential for rapid conduction of action potentials in the vertebrate nervous system. Of particular importance are the nodes of Ranvier, sites of voltage-gated sodium channel clustering that allow action potentials to be propagated along myelinated axons by saltatory conduction. Despite their critical role in the function of myelinated axons, little is known about the mechanisms that organize the nodes of Ranvier.

Results: Starting with a forward genetic screen in zebrafish, we have identified an essential requirement for *nsf* (N-ethylmaleimide sensitive factor) in the organization of myelinated axons. Previous work has shown that NSF is essential for membrane fusion in eukaryotes and has a critical role in vesicle fusion at chemical synapses. Zebrafish *nsf* mutants are paralyzed and have impaired response to light, reflecting disrupted *nsf* function in synaptic transmission and neural activity. In addition, *nsf* mutants exhibit defects in Myelin basic protein expression and in localization of sodium channel proteins at nodes of Ranvier. Analysis of chimeric larvae indicates that *nsf* functions autonomously in neurons, such that sodium channel clusters are evident in wild-type neurons transplanted into the *nsf* mutant hosts. Through pharmacological analyses, we show that neural activity and function of chemical synapses are not required for sodium channel clustering and myelination in the larval nervous system.

Conclusions: Zebrafish *nsf* mutants provide a novel vertebrate system to investigate Nsf function in vivo. Our results reveal a previously unknown role for *nsf*, independent of its function in synaptic vesicle fusion, in the formation of the nodes of Ranvier in the vertebrate nervous system.

Introduction

Myelin is an evolutionary adaptation that is necessary for rapid transmission of action potentials in vertebrates. Specialized glial cells—Schwann cells in the peripheral nervous system (PNS) and oligodendrocytes in the central nervous system (CNS)—repeatedly wrap their membranes around axons and form a densely compacted myelin sheath. Voltage-gated sodium channels are clustered at high concentrations within the nodes of Ranvier, periodic discontinuities in the myelin sheath where the axolemma is exposed to the extracellular environment [1]. Action potentials are propagated along axons at these nodes via saltatory conduction, which is much more efficient than continuous conduction in unmyelinated axons [1]. Because disruptions in myelin can lead to a range of neurological disorders, including multiple sclerosis, an understanding of mechanisms governing the form and function of myelinated axons is of clinical importance.

Numerous studies have suggested that signaling between neurons and glia is essential for myelination and node formation [1–3]. Data regarding other potential modulators of myelination, such as activity of the neurons themselves, are less clear. Depending on experimental conditions and organisms used, studies investigating possible relationships between neural activity and myelination in the CNS give contrasting results (reviewed in [4]), some indicating that neural activity enhances myelination and influences node formation [5], while others report that activity has no detectable effect. Fewer studies have focused on how neural activity may influence myelination in the PNS. In cultured cells, axons firing at low frequencies, but not those that are inactive or firing at faster frequencies, can delay Schwann cell differentiation in vitro [6, 7]. Because these studies were performed in cultured cells, and with a fairly specific range of axon firing rates, their relevance to physiological conditions is not firmly established. Less is known about possible roles of neural activity in regulating the organization of myelinated axons. There is some evidence that conduction velocities of certain myelinated axons are precisely tuned to coordinate signals coming from or going to different locations, suggesting that neural activity may feed back on axonal structure to modulate conduction velocity by regulating parameters such as axon diameter, myelin thickness, or node spacing [8]. Additional analysis of myelination in vivo will allow a more complete understanding of the relationship between neural activity and the organization of myelinated axons under physiological conditions.

To better understand the genetic mechanisms controlling the development of myelinated axons, we undertook a genetic screen for zebrafish mutants with abnormal myelin gene expression (H.-M.P., N. Sternheim, B. Diamond, D.A.L., I.G.W., and W.S.T., unpublished data). We show here that two mutations identified in our screen disrupt the zebrafish ortholog of N-ethylmaleimide sensitive factor (NSF), a protein essential for membrane fusion [9, 10]. NSF plays a key role in the nervous systems of both invertebrates and vertebrates by facilitating proper fusion of neurotransmitter-containing vesicles at synaptic termini, thereby allowing communication between neurons via chemical synaptic transmission [11–15]. Further studies have identified numerous binding partners for NSF aside from proteins acting in general membrane fusion. These studies have uncovered fusion-independent roles for NSF, the best characterized of which is the stabilization of the

*Correspondence: talbot@cmgm.stanford.edu

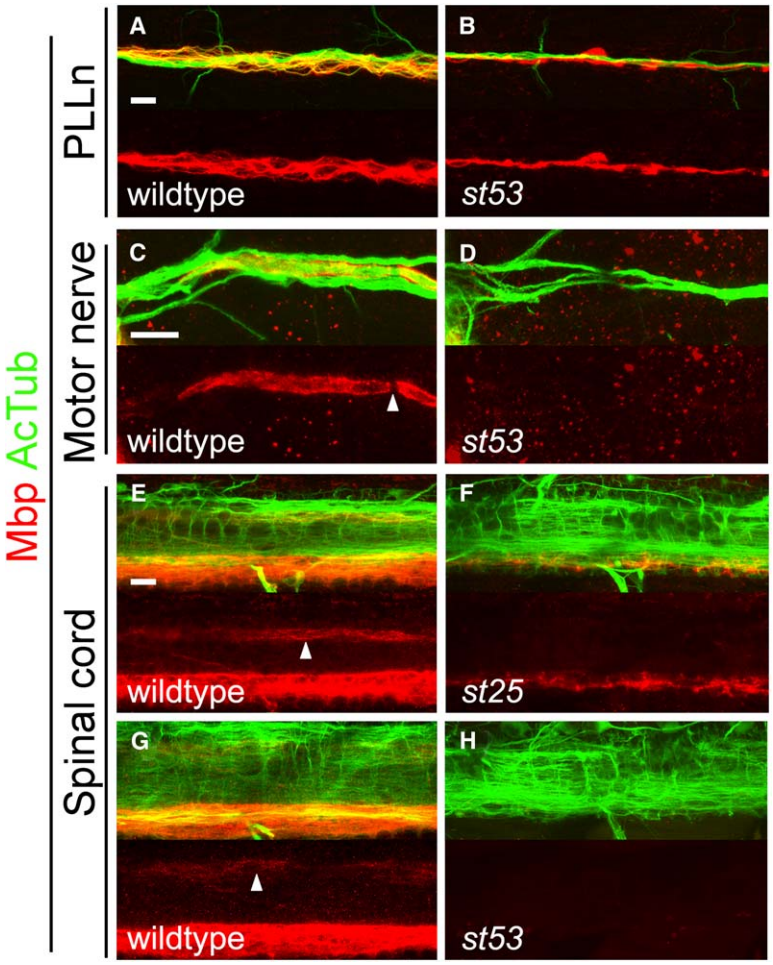

Figure 1. Reduced Expression of Myelin Basic Protein in *st25* and *st53*

(A and B) Images of double-label antibody staining preparations from the PLLn in larvae of the indicated genotypes at 5 dpf. Mutant larvae exhibited Mbp expression along nerve fibers that are thinner than in wild-type larvae. Mbp expression alone is shown below each corresponding double-label antibody image.

(C and D) Images of double-label antibody staining preparations from a motor nerve in larvae of the indicated genotypes at 5 dpf. Mutant larvae exhibited thin motor nerves that lacked Mbp expression. Mbp expression alone is shown below each corresponding double-label antibody image. The arrowhead in (C) marks a gap in Mbp expression at a putative node of Ranvier.

(E–H) Images of double-label antibody staining preparations from the spinal cord in larvae of the indicated genotypes at 5 dpf. Dorsal expression of Mbp, indicated by arrowheads in wild-type siblings (E, G), was absent in both mutants (F, H), and *st53* mutants (H) also lacked expression in the ventral spinal cord. Mbp expression alone is shown below each corresponding double-label antibody image. Scale bars equal 10 μm.

glutamate receptor subunit GluR2 at postsynaptic membranes (reviewed in [16]). As analyses of additional NSF binding partners are undertaken, the scope of NSF-associated activities apart from membrane fusion will likely be broadened further.

In addition to their myelination phenotypes, the zebrafish *nsf* mutants identified in our screen also show defects associated with lack of neural activity. Through pharmacological experiments, we show that neither action potentials nor chemical synaptic transmission is required for myelination or sodium channel clustering in zebrafish. In addition, analysis of genetic chimeras indicates that clustering of sodium channels at the nodes of Ranvier requires *nsf* function in neurons. Our data provide a new vertebrate loss-of-function model for NSF and demonstrate that *nsf* possesses a previously unrecognized neuronal role in myelination and node formation.

Results

st25 and *st53* Mutations Disrupt Development of Myelinated Axons

To better understand the molecular mechanisms underlying myelination, we undertook a forward genetic screen for zebrafish mutants with disrupted expression of *myelin basic protein* (*mbp*), which labels myelinating glial cells in zebrafish larvae (H.-M.P., N. Sternheim, B. Diamond, D.A.L., I.G.W., and W.S.T., unpublished data, [17]). Two of the mutations found in this screen, *st25* and *st53*, exhibited defects in *mbp* expression in glial cells of both the PNS and CNS (see Figure S1 in the Supplemental Data available with this article online). Mapping and complementation studies indicated that these two mutations disrupt the same gene (see below).

Immunofluorescence analyses with anti-Mbp antibodies revealed that a reduced level of Mbp was present in the posterior lateral line nerve (PLLn, Figures 1A and 1B). Mbp expression associated with motor nerves (MNs) was disrupted to a much greater extent in mutants (Figures 1C and 1D). Analysis of *foxd3::gfp* transgenic embryos, which express GFP in Schwann cells of the PLLn [18], indicated that Schwann cell development was normal in the PLLn of *st25* mutants through at least 48 hpf (Figure S1). By 96 hpf, a slight reduction in *foxd3::gfp* expression was evident in *st25* mutants (Figure S1), consistent with the reduction of Mbp in these mutants. In addition, axonal acetylated tubulin expression is reduced in the PLLn and MN of the mutants (Figures 1B and 1D). Reduction of Mbp was also evident in the CNS: in wild-type embryos, Mbp was present in dorsal and ventral tracts within the spinal cord (Figures 1E and 1G), while *st25* mutants lacked the dorsal Mbp expression (Figure 1F) and *st53* mutants lacked all Mbp

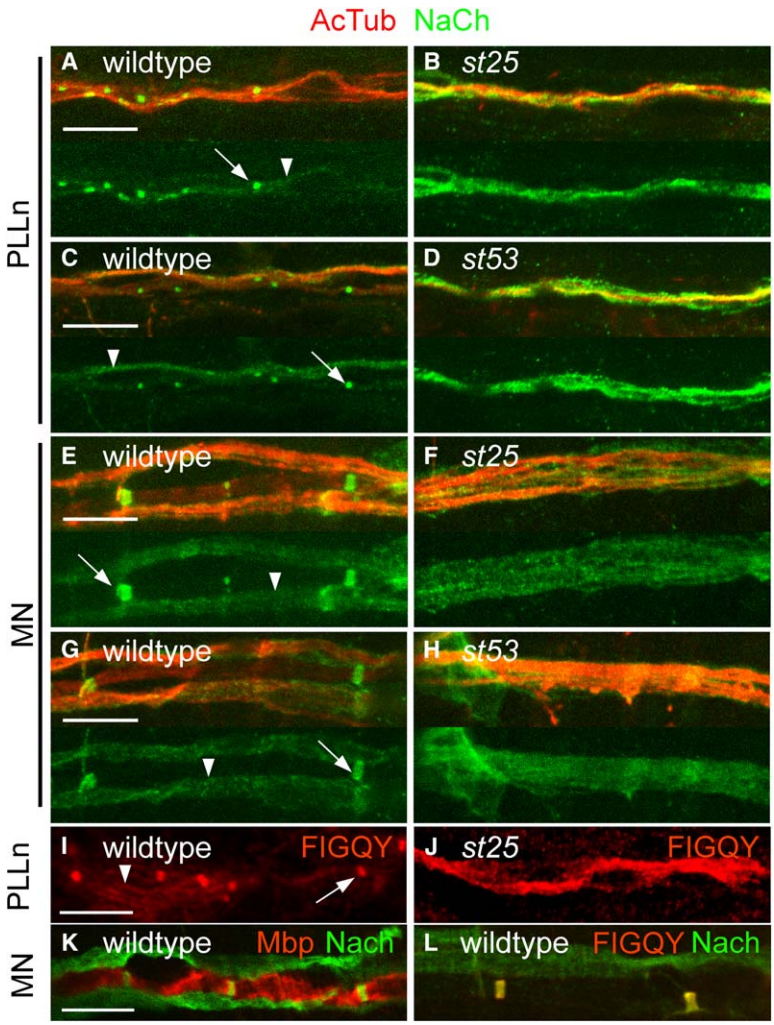

Figure 2. Defects in Organization of Myelinated Axons in *st25* and *st53*

(A–D) Images of double-label antibody staining preparations from the PLLn in larvae of the indicated genotypes at 5 dpf. In each panel, sodium channel (NaCh) antibody staining is shown alone below the corresponding double-label image. Individual axons, some of which are myelinated, are organized into a bundle in this nerve. Wild-type embryos showed labeling of sodium channels that was both diffuse (arrowheads) and clustered at discrete points along axons (arrows). Neither *st25* nor *st53* mutant larvae showed clustering of sodium channels in the PLLn.

(E–H) Images of double-label antibody staining preparations from motor nerves (MN) in larvae of the indicated genotypes at 5 dpf. At this stage, these nerves consist of one or two prominent axons usually situated between bundles of smaller axons. Wild-type larvae exhibited sodium channel clusters in the prominent axons (arrows) as well as diffuse labeling of sodium channels in neighboring axons (arrowheads), while mutant larvae lacked sodium channel clusters.

(I and J) FIGQY expression in PLLn of wild-type (I) and *st25* mutant (J) larvae. Wild-type larvae exhibited both diffuse FIGQY staining (arrowhead) and bright clusters of FIGQY labeling (arrow), while mutants exclusively exhibited diffuse FIGQY staining.

(K and L) Images of double-label antibody staining preparations of motor nerves at 5 dpf. In (K), sodium channel clusters (green) are localized at gaps in Mbp expression. In (L), sodium channel labeling colocalizes with FIGQY labeling at nodes of Ranvier. Scale bars equal 10 μm.

expression within the spinal cord (Figure 1H). No obvious defects were observed in axonal acetylated tubulin expression in the CNS (Figures 1F and 1H).

To further explore the defects in myelinated axons, we examined the nodes of Ranvier with a monoclonal antibody recognizing all voltage-gated sodium channels [19]. In whole-mount imunofluorescence analysis, this antibody labeled bright sodium channel (NaCh) clusters along some axons in peripheral nerves and produced diffuse staining along others (Figures 2A, 2C, 2E, and 2G). Similar results were observed in larvae labeled with antibodies against a sequence (FIGQY) conserved in neurofascin family adhesion molecules (Figure 2I), some of which (NrCAM, NF186) are known to localize to nodes in mammals [20]. Because of the colocalization of FIGQY antigen and NaCh clusters (Figure 2L) and because the NaCh clusters are complementary in expression with markers of internodes (Figure 2K), we conclude that these clusters define the positions of nodes of Ranvier along myelinated axons in larval zebrafish. The diffuse NaCh labeling represents unclustered sodium channels along the surface of unmyelinated axons. In contrast to wild-type larvae, *st25* and *st53* mutant larvae completely lacked sodium channel and FIGQY clusters, and instead exhibited diffuse labeling along the length of all axons in the PLLn and MN (Figures 2B, 2D, 2F, 2H, and 2J). Mutant larvae also lacked sodium channel clusters in the spinal cord (data not shown).

Background Adaptation and Motility Defects in *st25* and *st53*

Homozygous mutants died as early larvae and displayed pronounced neurological defects. Mutant larvae failed to respond to touch and had strongly reduced motility at 5 dpf (Figures 3E–3G; Figure S2). The motility phenotype of *st53* was more severe than that of *st25*, and the motility defects in both mutants were less severe at 3 dpf. The mutants also displayed a pigmentation phenotype characteristic of defects in the visual system [21]. At 4–5 dpf, melanophores of wild-type zebrafish larvae respond to the color tone of their environment by modulating their distribution of melanosomes in a process termed background adaptation. Larvae that are unable to perceive background tone respond as if raised in darkness and have fully expanded melanophores. Melanophore expansion was evident in both head and trunk regions of mutant larvae (Figures 3A–3D), suggesting that they cannot perceive or process visual stimuli.

In addition, mutant larvae failed to inflate their swim bladders, a phenotype commonly associated with larval

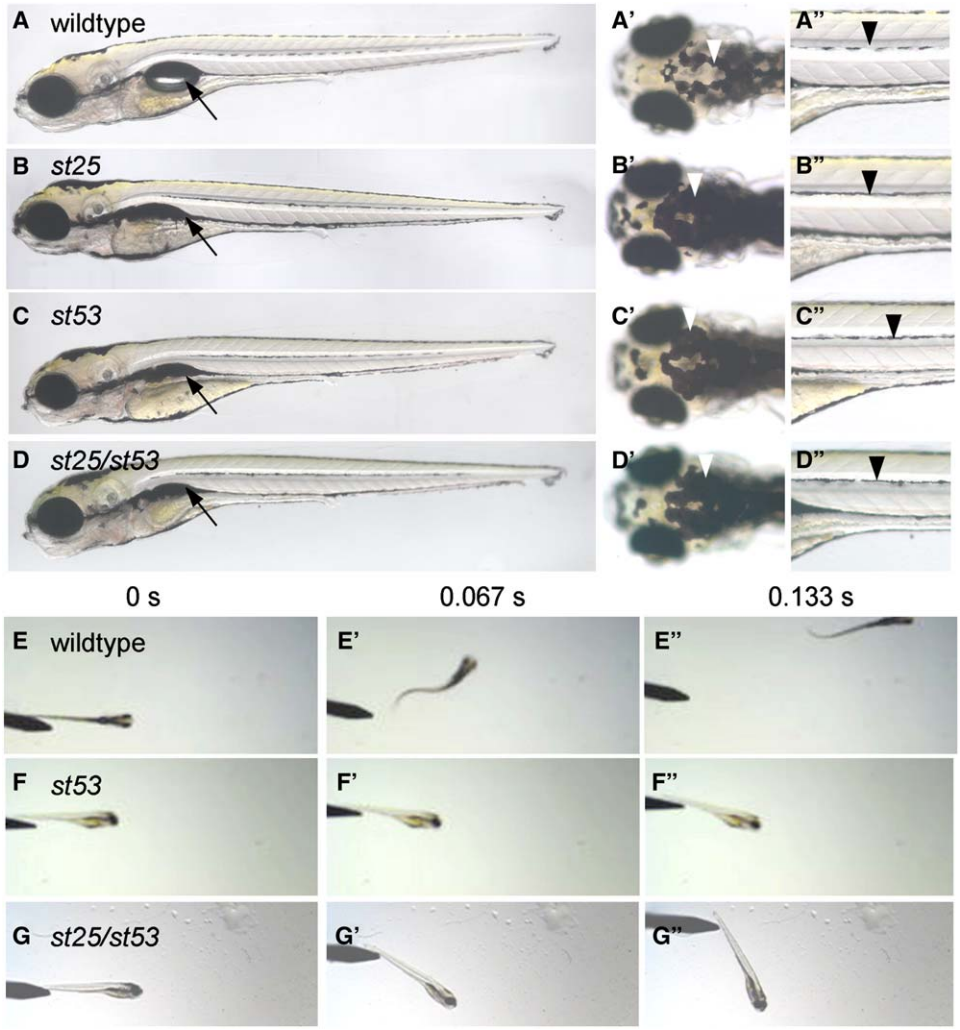

Figure 3. Background Adaptation and Motility Defects in *st25* and *st53*

(A–D) Images of live larvae at 5 dpf. Mutant homozygotes and transheterozygotes lacked swim bladders (arrows) and exhibited expanded pigment (arrowheads) in head (A′–D′) and trunk (A′′–D′′) regions. The eyes of *st53* mutants were slightly smaller than those of wild-type, *st25*, or transheterozygote larvae.

(E–G) Still images from movies of larvae at 5 dpf showing motility defects in mutant homozygote and transheterozygote larvae. Time elapsed between images is indicated.

lethal mutations in zebrafish (Figures 3B–3D). Aside from the lack of background adaptation and swim bladder inflation, mutant larvae appeared morphologically normal, although the eye size was slightly reduced in some *st53* mutant larvae (Figure 3C). *st25*/*st53* transheterozygotes also lacked swim bladders and exhibited motility defects, indicating that *st25* and *st53* fail to complement (Figures 3D and 3G).

Zebrafish *nsf* Is Disrupted by *st25* and *st53*

By using a positional cloning approach, we identified *N-ethylmaleimide sensitive factor* (*nsf*) as the gene disrupted by the *st25* and *st53* mutations (Figures 4A and 4B). Sequencing identified lesions in the *nsf* coding region of both *st25* and *st53* mutants (Figure 4C). In *st25*, a T to C transition is predicted to change a highly conserved leucine to a proline, while in *st53*, a C to A transversion introduces a premature stop codon into the *nsf* open reading frame (Figure 4D). Taken together, the mapping experiments, the identification of lesions, and RNA rescue experiments (see below) indicated that *nsf* is disrupted by the *st25* and *st53* mutations; accordingly, we refer to these mutations as nsf^{st25} and nsf^{st53}.

NSF is a member of the AAA ATPase family (ATPases associated with cellular activities) [22] and has three well-characterized functional domains: an N-terminal (N) domain that mediates interaction of NSF with SNAPs and SNAREs, an active ATPase domain (D1) that is responsible for its catalytic activity, and a catalytically inactive ATPase domain (D2) that mediates assembly of NSF monomers into a hexamer, the biologically active form of NSF (Figure 4D; [10, 16, 23, 24]). Zebrafish Nsf is highly conserved with NSF proteins in other vertebrates (85% identical, 93% similar to human Nsf, Figure S3). The nsf^{st25} lesion is within the D2 domain, and the predicted nsf^{st53} mutant protein is truncated prior to the D2 domain (Figure 4D). The substitution of proline for leucine at residue 630 in nsf^{st25} is predicted to

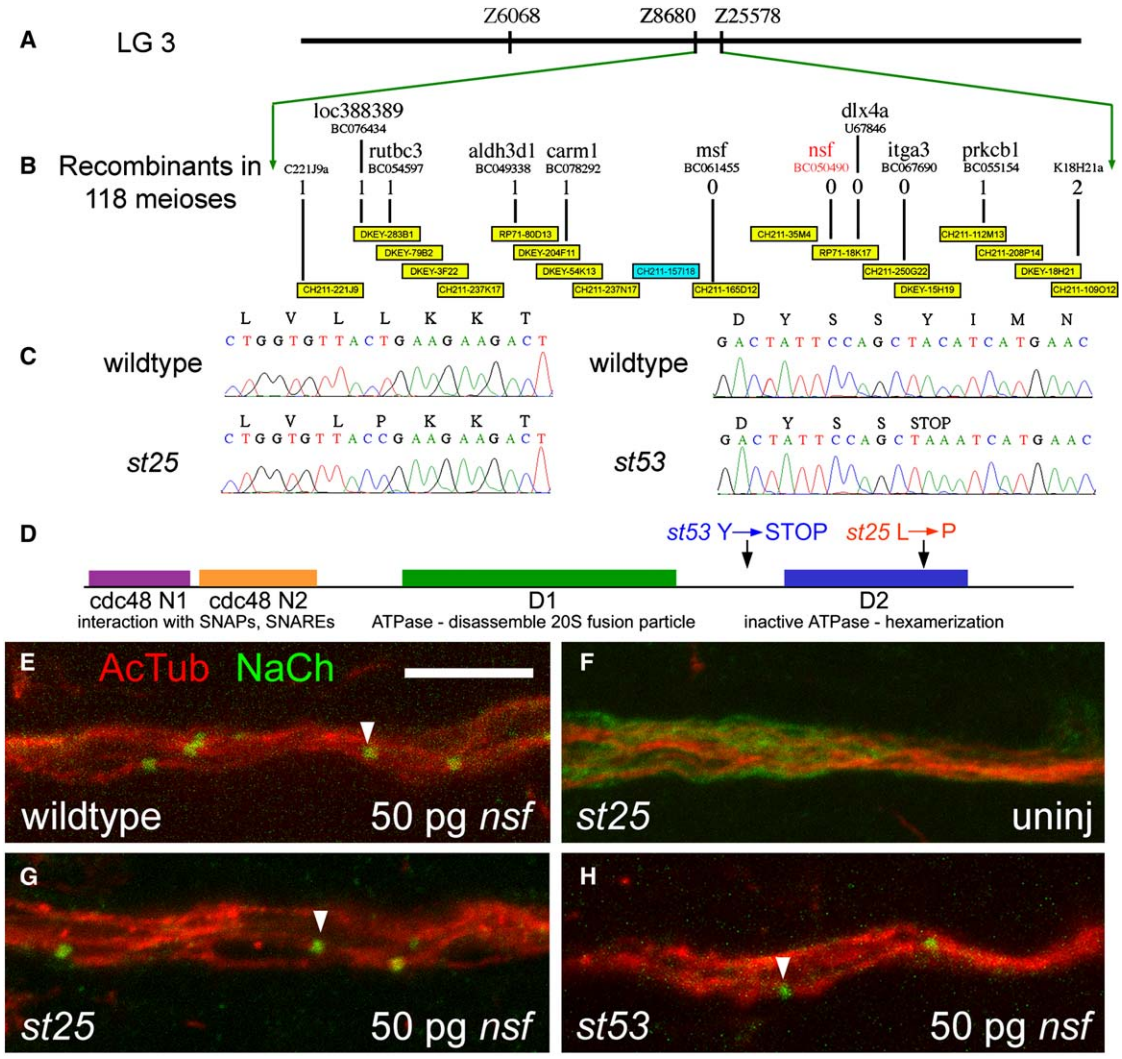

Figure 4. Positional Cloning of *st25* and *st53* and Rescue of the *st25* and *st53* Phenotype by *nsf* mRNA Injection

(A and B) Genetic and physical map of the *st25* and *st53* region of LG 3, showing BACs spanning the region, and genetic markers used to refine the *st25* interval. Sequence information was available for all BACs shown in yellow. Four polymorphisms in genes within these BACs, including a polymorphism in *nsf*, showed zero recombinants with *st25* among 118 meioses.

(C) Sequence traces from homozygous wild-type, *st25*, and *st53* mutant larvae. The *st25* lesion changes a conserved leucine to a proline, while the *st53* lesion introduces a premature stop codon into the open reading frame.

(D) Model of Nsf protein structure. The *st25* lesion occurs in the D2 domain, while the *st53* lesion introduces a premature stop in the open reading frame prior to the D2 domain.

(E–H) Images representing double-label antibody staining preparations of the PLLn of larvae of the indicated genotypes and injection treatments at 72 hpf. Antibodies used are acetylated tubulin (red) and the sodium channel (NaCh) antibody (green).

(E) Wild-type siblings injected with 50 pg of synthetic *nsf* mRNA show normal clustering of sodium channels (arrowheads) along axons.

(F) Uninjected mutant larvae lacked sodium channel clustering and exhibited diffuse labeling of sodium channels along axons.

(G and H) Mutants injected with 50 pg of synthetic *nsf* mRNA showed rescue of sodium channel clustering (arrowheads). Scale bar equals 10 μm.

disrupt an α helix that contains residues thought to contribute to stabilization of NSF-D2 protomers; in addition, this substitution occurs immediately prior to a lysine (residue 631) that may be important for interactions between ATP and the D2 domain [25, 26]. Moreover, additional database searches revealed that zebrafish possesses a duplicate *nsf* gene (*nsfb*, Figure S3).

Rescue of nsf^{st25} and nsf^{st53} by mRNA Injection

To obtain additional evidence that *nsf* is disrupted by the nsf^{st25} and nsf^{st53} mutations, we rescued the mutants by injecting synthetic wild-type *nsf* mRNA. Injection of approximately 50 pg of *nsf* RNA into wild-type embryos did not obviously affect the number or morphology of sodium channel clusters in the PLLn (Figure 4E). Whereas all uninjected *nsf* mutants lacked sodium channel clusters in the PLLn (Figure 4F), some mutants injected with approximately 50 pg of wild-type *nsf* mRNA exhibited rescue of sodium channel clustering. Rescue was more efficient for nsf^{st25} individuals: 85% (46 of 54) of injected nsf^{st25} homozygotes exhibited sodium channel clustering in the PLLn (Figure 4G), compared to 36% (16 of 45) of injected nsf^{st53} homozygotes (Figure 4H).

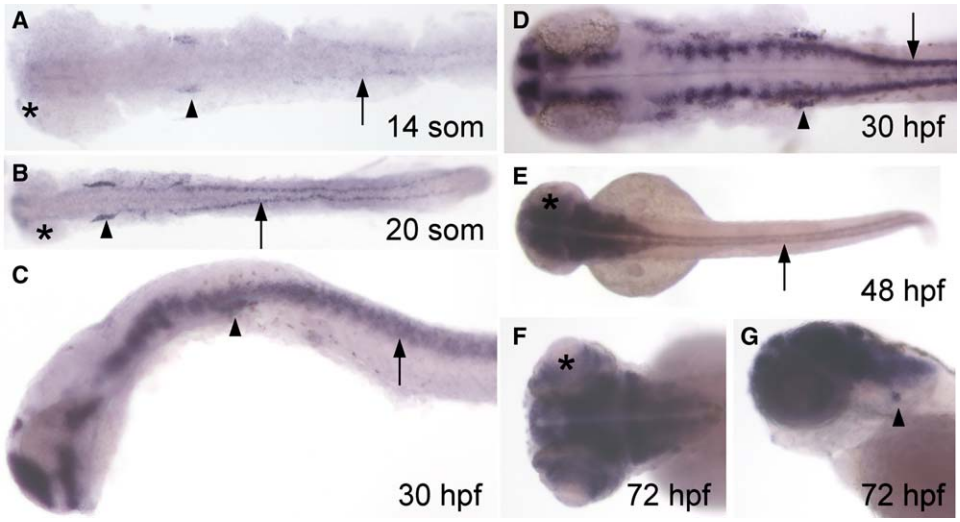

Figure 5. Expression of *nsf* Examined by In Situ Hybridization

(A) Dorsal view of a flat-mount embryo at 14 somites (16 hpf) showing *nsf* expression in the developing forebrain region (asterisk), trigeminal ganglia (arrowhead), and spinal cord (arrow). In addition, *nsf* transcripts were detectable by RT-PCR at 2 hpf, prior to the zebrafish midblastula transition (not shown).

(B) Dorsal view of a flat-mount embryo at 20 somites (19 hpf), showing continuing expression of *nsf* in the forebrain (asterisk), in the trigeminal ganglia (arrowhead) and other cranial ganglia, and in the spinal cord (arrow) along the length of the trunk and tail.

(C) Lateral view of an embryo at 30 hpf showing expression of *nsf* in the brain, the posterior lateral line ganglion (PLLg, arrowhead), and along the length of the spinal cord (arrow).

(D) Dorsal view of an embryo at 30 hpf showing expression in the brain, in cranial ganglia including the PLLg (arrowhead), and bilaterally along the spinal cord (arrow).

(E) At 48 hpf (dorsal view), *nsf* transcripts are visible in the eyes (asterisk), brain, and along the length of the spinal cord (arrow).

(F) Dorsal view at 72 hpf, showing expression of *nsf* in the eyes (asterisk) and throughout the brain.

(G) Lateral view at 72 hpf showing *nsf* expression in the PLLg (arrowhead). Anterior is to the left in all images.

Expression of *nsf* in Embryonic and Larval Zebrafish

Although expression of *nsf* was not visible by whole-mount in situ hybridization at early embryonic stages, *nsf* mRNA was detectable throughout embryogenesis by RT-PCR as early as 2 hpf (data not shown). Like mammalian *Nsf* [27], zebrafish *nsf* is primarily expressed in the developing nervous system. At the 14 somite stage, *nsf* is expressed within cells of the developing trigeminal ganglia, anterior spinal cord, and forebrain (Figure 5A). At 20 somites, transcripts were detectable in additional cranial ganglia and throughout the length of the developing spinal cord (Figure 5B). By 30 hpf, *nsf* was also visible in regions of the developing midbrain and hindbrain, and in the posterior lateral line ganglia (Figures 5C and 5D). At 48 hpf, expression persisted in the spinal cord and was present throughout most of the developing brain and eyes (Figure 5E), while at 72 hpf, spinal cord expression was less evident (Figures 5F and 5G). Expression in the posterior lateral line ganglia persisted to at least 72 hpf (Figure 5G).

Sodium Channel Clustering Requires *nsf* Function in Neurons

Though our analysis suggests that *nsf* RNA is expressed predominantly in neurons, a previous study reported specific localization of NSF protein to microvilli of myelinating Schwann cells in mice, suggesting a possible role for Nsf in glia [28]. To determine whether *nsf* function is required in neurons or Schwann cells, we created chimeric embryos wherein wild-type cells were transplanted into nsf^{st53} mutant embryos at early blastula stages. In four such chimeras, sodium channel clusters were observed along PLLn axons of neurons derived from wild-type donors (Figure 6). Furthermore, no wild-type glia were associated with these axons, and sodium channel clusters were seen only along axons of wild-type donor neurons. Similar autonomous rescue of sodium channel clustering was observed in the spinal cord in three additional chimeras (data not shown). These results indicate that *nsf* functions autonomously in neurons to cluster sodium channels at nodes of Ranvier.

Voltage-Gated Sodium Channel Activity Is Not Required for Myelination or Sodium Channel Clustering

To determine whether the myelination defects observed in the *nsf* mutants result from lack of general neural activity, we injected zebrafish embryos at 26–30 hpf with tetrodotoxin (TTX), which blocks voltage-gated sodium channels and disrupts action potentials [29–31]. TTX-treated larvae were paralyzed through 5 dpf (Figures 7A and 7B) and exhibited defective background adaptation (Figure S4). In contrast to the *nsf* mutants, TTX-treated larvae exhibited robust expression of Mbp protein in almost all regions (Figures 7C–7F, Figure S4). Expression of Mbp, however, was not evident in a small number of motor nerves in a subset of TTX-treated larvae (data not shown). Moreover, TTX-treated and control larvae exhibited a similar number of sodium channel clusters along axons in both the PNS (Figures 7G–7K) and CNS (not shown). In a separate experiment, embryos were injected with TTX before the 8 cell stage

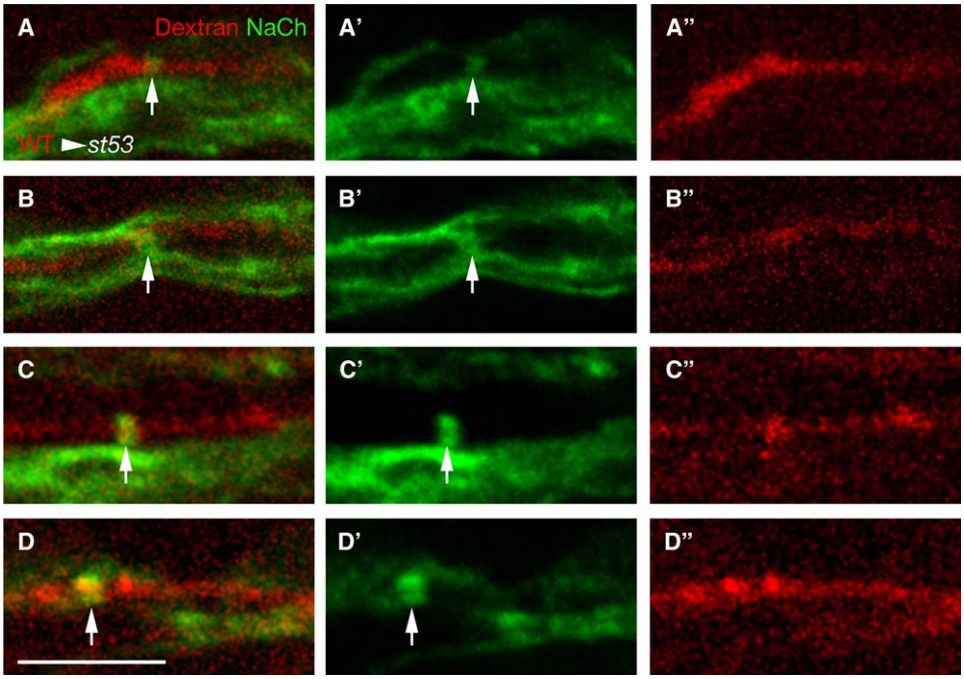

Figure 6. Clustering of Sodium Channels Requires *nsf* Function in Neurons

Chimeric larvae generated by transplanting dye-labeled wild-type cells into *nsf*^{st53} mutants were analyzed to detect sodium channel proteins (green) and the dye label (red). Sodium channel expression (A′–D′), the dye-labeled axons (A′′–D′′), and a merged image (A–D) are shown for four different examples from three different chimeras. In these examples, all of the wild-type cells in the PLLn were neurons, and nodal sodium channel clusters were evident only on wild-type axons. Arrows indicate nodal sodium channel clusters. The genotype of phenotypically mutant host embryos was confirmed by PCR. Scale bar equals 10 μm.

and assayed with markers of myelination as above; these larvae were similar to those injected at 26–30 hpf (data not shown).

Node Formation in the PLLn Does Not Require Functional Hair Cells

Because NSF has a well-described and essential role in the release of neurotransmitters at synapses [11–15], we sought to determine whether the myelination defects in *nsf* mutants were caused by disrupted communication from presynaptic inputs. To investigate this possibility, we analyzed node formation in the PLLn, which contains bipolar neurons that receive synaptic inputs from hair cells of the lateral line and send central projections to the hindbrain. Hair cells are acutely sensitive to aminoglycoside antibiotics such as neomycin. Low doses of these antibiotics block hair cell function [32], whereas higher doses of neomycin cause hair cell death [33]. To investigate the role of hair cell activity in PLLn node formation, we treated zebrafish larvae with neomycin, ranging in concentration from 0.5 mM, which has been demonstrated to kill almost all hair cells in larval zebrafish [33], to 2 mM, a dose that is lethal for most treated larvae by 5 dpf. Acetylated tubulin labeling of treated larvae confirmed that hair cells were severely reduced or absent (Figures 8A and 8B). Analysis of sodium channel clustering in the PLLn of treated larvae, however, did not reveal significant differences in cluster formation or number at 0.5 mM neomycin or at higher doses (80 hpf: $p > 0.05$; 5 dpf: 0.5 mM/$p > 0.05$; 1 mM/$p > 0.05$; 2 mM/$p > 0.05$; Figures 8C, 8D, and 8N), indicating that hair cell loss did not disrupt formation of nodes in the PLLn.

Node Formation Does Not Require Chemical Synaptic Activity

While neomycin treatment caused a strong reduction in hair cell number, hair cells were not entirely eliminated at high doses of neomycin (Figure 8B, [33]), leading to the possibility of residual synaptic function. To further investigate a potential influence of synaptic activity upon myelination, we injected embryos with botulinum neurotoxin B (BoNT/B), which selectively cleaves the v-SNARE synaptobrevin and abolishes neurotransmitter release [34] and has been shown to block chemical synaptic activity in zebrafish [35]. Treated larvae were raised to 5 dpf; 50 pg of the toxin was sufficient to induce paralysis throughout development (Figure 8E).

Larvae treated with either 50 pg or 500 pg of toxin exhibited sodium channel clusters in the PLLn at 72 hpf, suggesting that chemical synaptic transmission is not required for node formation. The lower dose was sufficient to induce paralysis, but there was no significant reduction in sodium channel cluster number in the PLLn at 3 dpf (50 pg: $p > 0.05$, Figure 8N). At the higher dose, which was 10 times higher than needed to induce paralysis, there was a slight but significant reduction in sodium channel cluster number in the PLLn at 3 dpf (500 pg: $p = 0.03$). It is unclear whether the node reduction at the higher dose is specific to the effects of the toxin on chemical synaptic transmission, or if it might result from developmental delay or poor health of treated

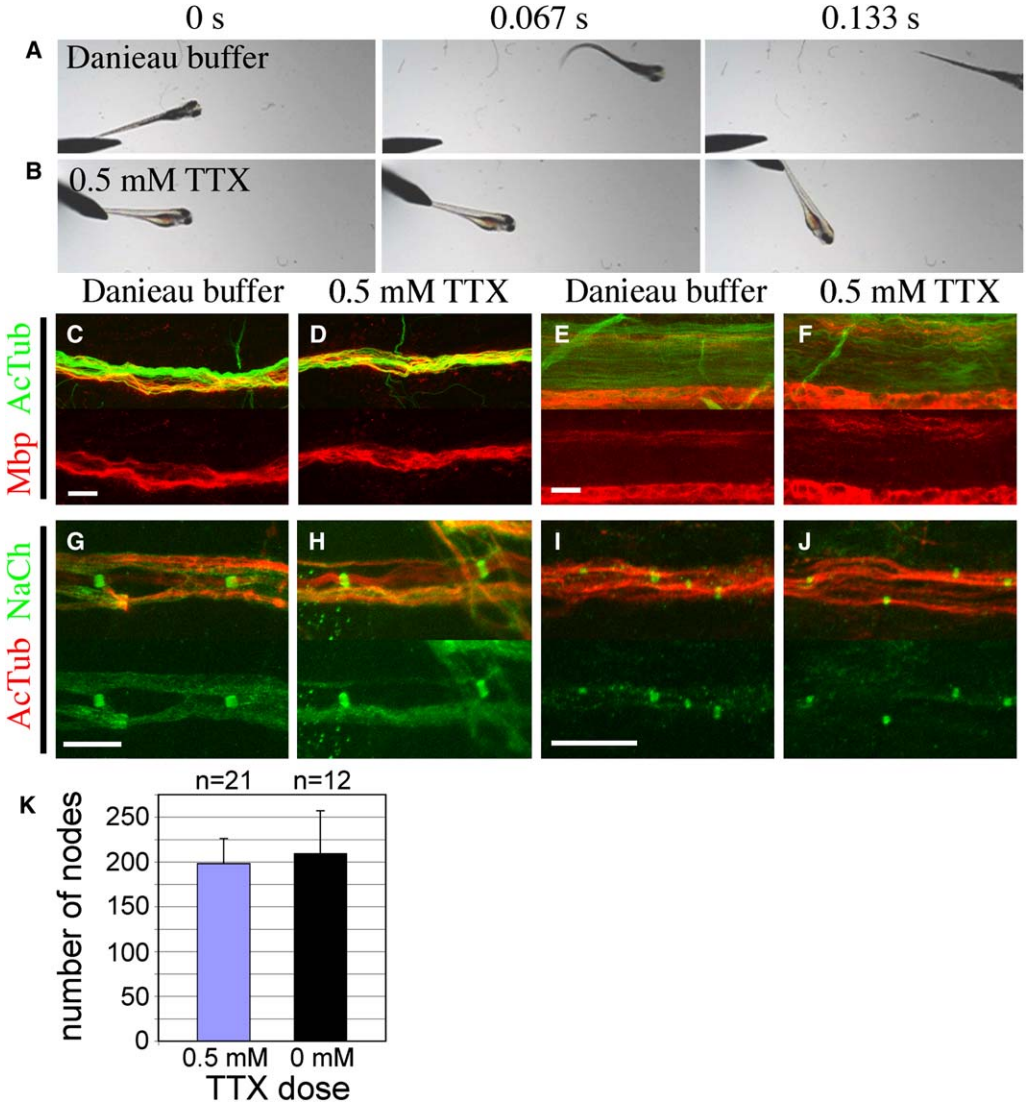

Figure 7. Neural Activity Is Not Required for Myelination or Clustering of Sodium Channels along Axons

(A and B) Still images from movies showing paralysis of TTX-treated larvae at 5 dpf. Time elapsed between images is indicated.

(C and D) Images from double-label antibody staining preparations showing normal Mbp expression associated with the PLLn in TTX-treated larvae at 5 dpf. Mbp expression alone is shown below the corresponding double label image.

(E and F) Images from double-label antibody staining preparations showing normal Mbp expression in the spinal cord of TTX-treated larvae at 5 dpf. Mbp expression alone is shown below the corresponding double label image.

(G and H) Images from double-label antibody staining preparations showing normal clustering of sodium channels in motor nerves of TTX-treated larvae. NaCh expression alone is shown below the corresponding double label image.

(I and J) Images from double-label antibody staining preparations showing normal clustering of sodium channels in the PLLn of TTX-treated larvae at 5 dpf. NaCh expression alone is shown below the corresponding double label image.

(K) Quantitation of sodium channel cluster number in the PLLn of control and TTX-treated larvae at 5 dpf. Error bars denote standard deviation. The difference in node number was not statistically significant ($p > 0.05$). Scale bars equal 10 μm.

larvae, a subset of which exhibited slow heartbeats, heart edemas, and reductions in head and eye size. Sodium channel clusters were also present in motor nerves (Figures 8H and 8I) and in the spinal cord of treated larvae at 5 dpf, but heavy pigmentation along the lateral line in treated larvae, presumably arising because of defects in background adaptation, precluded quantitation of node number at this stage. In addition, toxin-treated larvae exhibited Mbp expression along the LLn, motor nerves, and spinal cord (Figures 8J–8M). Moreover, toxin-treated larvae exhibited reduced acetylated tubulin expression in the PLLn at 5 dpf, similar to *nsf* mutants (data not shown). These experiments indicate that loss of synaptic function leads to defects in motility and background adaptation, but does not affect myelination or clustering of sodium channels at the nodes of Ranvier.

Neural Cell Death in nsf^{st25}, nsf^{st53}, and BoNT/B-Treated Larvae

Because the PLLn was reduced in both *nsf* mutants and BoNT/B larvae, we wished to assess neural cell

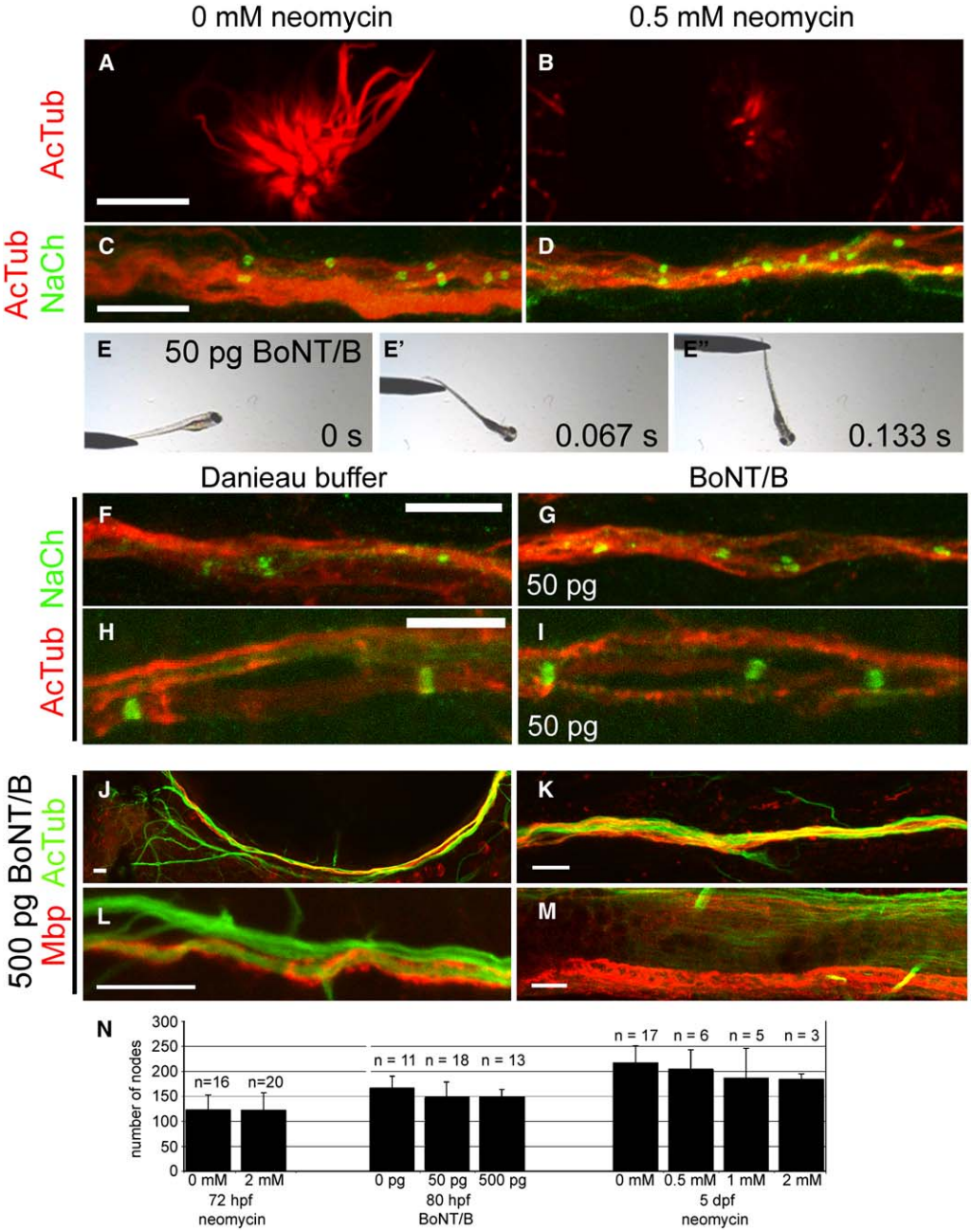

Figure 8. Synaptic Activity Is Not Required for Myelination or Clustering of Sodium Channels along Axons

(A and B) Acetylated tubulin labeling of hair cells in wild-type and neomycin-treated larvae at 5 dpf. Neomycin-treated larvae showed severe reduction of hair cells.

(C and D) Images from double-label antibody staining preparations showing normal clustering of sodium channels in the PLLn of neomycin-treated larvae at 5 dpf.

(E) Still images from a movie showing paralysis of BoNT/B-treated larvae at 5 dpf. Time elapsed between images is shown. Toxin-treated larvae also showed defects in background adaptation (not shown).

(F and G) Images from double-label antibody staining preparations showing normal clustering of sodium channels in the PLLn of BoNT/B-treated larvae at 80 hpf.

(H and I) Images from double-label antibody staining preparations showing normal clustering of sodium channels in the MN of BoNT/B-treated larvae at 5 dpf.

(J–M) Images from double-label antibody staining preparations showing normal expression of Mbp in the ALLn (J), PLLn (K), MN (L), and spinal cord (M) of BoNT/B-treated larvae at 5 dpf. Scale bars equal 10 μm.

(N) Number of nodal sodium channel clusters in the PLLn of treated embryos at the indicated times. Error bars denote standard deviation.

death under these conditions. In the PNS, we assessed neuronal cell number by counting HuC-expressing cells in the PLLg at 72 hpf, when sodium channels have already begun to form clusters (Figure 4). This analysis showed slight but not statistically significant reductions in both *nsf* mutants (Figure S5). Like *nsf* mutants,

BoNT/B-treated embryos have reduced axonal tubulin staining in the PLLn, but counts of HuC-labeled neurons in the PLLg revealed no significant differences between toxin-treated and control larvae at 72 hpf (Figure S5), though cell number in the PLLg could not be assessed in a subset of toxin-treated larvae because of lack of robust HuC labeling.

In the CNS, acridine orange staining at 72 hpf detected little cell death in the wild-type spinal cord in the region adjacent to somites four through ten (Figure S5). In contrast, *nsf* mutants exhibited elevated levels of cell death in similar regions. Acridine orange labeling also revealed increased cell death in the spinal cord of BoNT/B-treated larvae at 3 dpf (Figure S5). These results indicate that survival of a small number of cells in the spinal cord requires *nsf* function and synaptic activity. Our data therefore indicate that both *nsf* and synaptic activity are required for axonal morphology and survival of some neurons. Because BoNT/B-treated larvae have nodal sodium channel clusters, we conclude that the role of *nsf* in organizing the node of Ranvier is independent of its function in synaptic vesicle fusion.

Discussion

By using the zebrafish model system, we have investigated the organization of developing myelinated axons in vivo. In a forward genetic screen, we have identified two mutations in *nsf* that reduce the expression of *myelin basic protein* in both the PNS and CNS of larval zebrafish. Moreover, nodes of Ranvier failed to form in *nsf* mutants, as visualized with antibodies against voltage-gated sodium channels and neurofascin family adhesion molecules. Confirmation that these mutations disrupted *nsf* was provided by identification of lesions in the *nsf* open reading frame and rescue of the mutant phenotype by injection with synthetic *nsf* mRNA. Visual perception and motility are impaired in the mutants, likely resulting from disruption of NSF function in neurotransmitter release at synapses. These *nsf* mutants will facilitate in vivo studies of NSF function in vertebrate synaptic transmission. In addition, via analyses of genetic chimeras and larvae treated with pharmacological inhibitors of synaptic transmission and action potentials, we have uncovered a new role for *nsf* in neurons, independent of its function in synaptic transmission, in organizing myelinated axons.

Role of NSF in Membrane Fusion and Synaptic Transmission

NSF was initially identified through its ability to restore transport between Golgi cisternae in a cell-free system wherein membrane fusion had been disrupted by the sulfhydryl alkylating agent N-ethylmaleimide [9]. Orthologs of NSF are present throughout eukaryotes and are thought to facilitate membrane fusion in all cells by disassembling SNARE complexes and possibly priming SNARE proteins for fusion, thereby maintaining a readily available pool of SNARE proteins for further fusion events [36]. In addition to its function in constitutive membrane fusion, NSF plays a key role in synaptic transmission, where it is required for fusion of neurotransmitter-containing vesicles with presynaptic membranes [11–15]. Zebrafish Nsf is highly similar (over 90%) at the amino acid level with other vertebrate NSF orthologs. In addition, like NSF in other vertebrates [27] and *Dnsf1* in *Drosophila* [37], zebrafish *nsf* is expressed primarily in the nervous system.

Given the role of NSF in constitutive membrane fusion, it was surprising that zebrafish *nsf* mutants were largely normal in morphology, with mutant phenotypes predominantly observed in the nervous system. The absence of defects in most cell types suggests that *nsf* function in general membrane fusion may be effected by maternally supplied transcripts or the duplicate *nsf* gene. Such partitioning of *nsf* function is observed in *Drosophila*, which also possesses two *nsf* genes [38, 39]. As in other cases where zebrafish duplicates function in different stages and cell types [40], partitioning of NSF roles between the zebrafish duplicates may facilitate precise context-dependent dissection of NSF function in vertebrates.

Requirement for NSF in Synaptic Transmission

Drosophila adults homozygous for the temperature-sensitive mutation *comatose*, which disrupts *nsf* function in the nervous system [12, 39], are paralyzed at restrictive temperatures [41]. Ultrastructural analysis of synapses in mutant flies showed accumulation of docked synaptic vesicles, indicating that neurotransmitter-mediated synaptic transmission is impaired in these mutants [14]. The zebrafish *nsf* mutants were similarly paralyzed, suggesting that disrupted synaptic transmission caused this aspect of the mutant phenotype. In addition, *nsf* mutants exhibited a background adaptation defect, which is an indicator of impaired visual function. Both the motility defects and background adaptation phenotypes were also induced by pharmacological inhibition of action potentials by TTX and of synaptic transmission by BoNT/B. These results indicate that defects in motility and the visual system in *nsf* mutants arise from disruption of the essential function of NSF in synaptic transmission and neural activity. Our analysis of *nsf* mutants and toxin-treated larvae indicates that only a small number of neurons in the larval nervous system require synaptic function and neural activity for survival.

Synapse-Independent Neuronal Requirement for *nsf* in Organizing the Node of Ranvier

There are at least two possible explanations for disruption of nodes of Ranvier in *nsf* mutants. First, there could be a previously undefined requirement for synaptic function in establishing the nodes of Ranvier. Second, NSF could have a novel role in organizing myelinated axons that is independent of synaptic function and neural activity. Such a role is not without precedent, as recent studies have defined binding partners and activities of NSF that do not relate to its role in membrane fusion [16]. The functional consequences of most of these interactions are not clear, but current evidence points to possible roles for NSF in intracellular transport or regulation of target protein expression at the cell surface. An intriguing parallel to the requirement of *nsf* in sodium channel localization to nodes is the finding that certain voltage-gated calcium channels require interaction with SNARE proteins—key substrates of NSF—for localization to synapses [42].

To investigate the role of Nsf in myelinated axons, we focused on the posterior lateral line nerve (PLLn), a prominent myelinated nerve in the PNS. The expression pattern of *nsf* indicated that it likely functions in PLLg neurons, and the primary defect observed in the PLLn of *nsf* mutants was a lack of sodium channel clusters at the nodes of Ranvier. Although *mbp* mRNA expression is reduced in the PLLn of *nsf* mutants, Schwann cells in *nsf* mutants appeared largely normal through 3 dpf and Mbp-expressing Schwann cells were present along axons until 5 dpf, well after the time when sodium channels normally cluster at nodes. Analysis of genetic chimeras demonstrated that *nsf* functions autonomously in neurons: nodal sodium channel clusters form in wild-type neurons transplanted into *nsf* mutant hosts. These results identify Nsf as a neuron-intrinsic factor with an essential function in establishing the nodes of Ranvier. Based on specific localization of Nsf protein to microvilli of myelinating Schwann cells, a previous study [28] proposed that NSF may function in glia to facilitate organization of nodes. Our analysis of genetic chimeras suggests that *nsf* functions primarily in neurons to establish nodal sodium channel clusters, but does not exclude other potential roles for *nsf* in glia.

To determine whether the myelination defects resulted from impaired NSF function in synaptic transmission, we employed pharmacological approaches to disrupt specific aspects of PLLn activity. TTX treatment did not induce defects in sodium channel clustering or Mbp expression in the PLLn, indicating that neural activity is not required for these aspects of myelination. To further dissect the role of *nsf* in node formation, we blocked communication from presynaptic inputs via two separate pharmacological treatments. Neomycin-induced hair cell loss had no obvious effect on sodium channel clustering. In addition, we blocked chemical synaptic transmission throughout larvae with botulinum neurotoxin B (BoNT/B). Like *nsf* mutants, BoNT/B-treated larvae had reduced PLLn nerves. The BoNT/B-treated larvae, however, exhibited normal sodium channel clustering and Mbp expression. Because the *nsf* mutants display phenotypes not observed in TTX or BoNT/B-treated larvae, we conclude that the requirement of *nsf* in the organization of nodes of Ranvier is independent of its role in chemical synaptic transmission and neural activity.

Neural Activity and Myelination

Numerous studies have suggested that activity of neurons may influence myelination. Depending on experimental context, these studies have reported conflicting results for the requirement of neural activity in the development of CNS myelin [4]. Fewer studies have focused on the role of activity in PNS myelination; these suggest that certain frequencies of axonal firing can inhibit Schwann cell differentiation in cultured cells [6]. It has also been proposed that neural activity may regulate the establishment of the nodes of Ranvier in myelinated axons [8]. In this study, we have demonstrated that neither elimination of action potentials nor inhibition of chemical synaptic transmission appreciably affected myelin gene expression or organization of nodes of Ranvier in developing zebrafish. Results of these pharmacological studies, therefore, indicate that neural activity is not required to initiate myelination in the developing CNS or PNS. Our experiments do not, however, rule out possible roles for neural activity in maturation or fine adjustments of myelinated axons. Further studies of myelination in zebrafish will clarify the relationship between neural activity and tuning of myelinated axons.

Conclusions

The mutants described in this study provide a novel model for study of *nsf* function in vertebrates. Zebrafish *nsf* mutants are paralyzed and have impaired visual function, reflecting the essential role of *nsf* in synaptic transmission and neural activity. Strikingly, the *nsf* mutants also exhibited failure of sodium channel clustering along myelinated axons at the nodes of Ranvier. Analysis of genetic chimeras indicated that *nsf* functions within myelinating axons to organize these specialized domains. Pharmacological inhibition of neural activity and chemical synaptic transmission phenocopied the motility and visual defects observed in *nsf* mutants. Clustering of sodium channels at the nodes of Ranvier, however, was largely normal in toxin-treated embryos. These results reveal a new role for *nsf* in neurons, independent of its role in synaptic activity, in the organization of the nodes of Ranvier.

Experimental Procedures

Fish Strains

Zebrafish embryos were raised at 28.5°C and were staged according to [43]. The *nsf*^{st25} and *nsf*^{st53} mutations were identified in a screen for ENU-induced mutations that disrupt expression of *mbp* at 5 dpf (H.-M.P., N. Sternheim, B. Diamond, D.A.L., I.G.W., and W.S.T., unpublished data). The *foxd3::gfp* strain was kindly provided by D. Gilmour [18].

Genetic Mapping and Positional Cloning of *nsf*^{st25} and *nsf*^{st53}

The *st25* and *st53* mutations were genetically localized via bulked segregant analysis with PCR-based simple sequence length polymorphisms (SSLPs) via standard methods [44]. Fully sequenced BACs within the *st25* interval were identified from the zebrafish fpc database (http://www.sanger.ac.uk/Projects/D_rerio/WebFPC/zebrafish). Predicted coding regions of these BACs were employed in additional mapping experiments to further refine the *st25* interval. Genomic DNA fragments from the *nsf* region of multiple *st25*, *st53*, and wild-type sibling embryos were amplified and sequenced to identify the lesions in the two alleles.

To genotype individual larvae in the phenotypic analyses, the *st25* mutation was scored in genomic DNA samples via an *Acu*I length polymorphism at the location of the *st25* lesion (primers, 5′-AAAAATGCTAATTGTTGGAATGA-3′ and 5′-AACGTAGTATAACT TGGGTTTTTGC-3′); similarly, *st53* individuals were genotyped with an *Rsa*I polymorphism at the *st53* lesion (primers, 5′-CAACCAAGA GGACTATTCCAGGTA-3′ and 5′-AGAGAGCTCACCCTCCAGAA-3′).

Microinjections and Transplantations

For the rescue experiments and the botulinum toxin experiments, embryos were injected through their chorions with approximately 500 pL of solution at the 1–4 cell stage. Synthetic *nsf* mRNA was generated with the SP6 mMessage mMachine kit (Ambion) after linearization with *Not*I and was diluted in 0.2 M KCl with 5 mg/mL Phenol Red prior to injection. Botulinum toxin (Calbiochem) was injected into embryos in 1 μg/μL or 0.1 μg/μL solutions as previously described [35]. Embryos that were immotile and lacked severe morphological defects at 5 dpf were selected for further analysis. Tetrodotoxin (TTX) was injected in a 0.5 mM solution in 1× Danieau buffer with 5 mg/mL Phenol Red. Embryos between 26 and 30 hpf were anesthetized in 0.016% (w/v) Tricaine and immobilized in 1.5% low melting point agarose, and TTX or control solutions were injected into eye or tectal regions. Larvae that were immotile at 5 dpf were

selected for further analysis. Transplantation experiments were performed as described previously [45].

In Situ Hybridization and Fluorescent Antibody Labeling

In situ hybridization was performed with standard protocols. The *mbp* probe has been described previously [46]. A full-length *nsf* cDNA (GenBank accession BC050490) in the pME18S vector was obtained from Open Biosystems. This cDNA was subcloned by high-fidelity PCR into the pCS2+ expression vector and was resequenced to ensure that no errors were introduced by PCR. Riboprobes were generated by linearizing this construct with *Hind*III, followed by polymerization with T7 RNA polymerase.

The sodium channel antibody (Sigma, clone K58/35, 1:500 [19]), the FIGQY antibody (gift of M. Rasband, 1:1000), and the acetylated tubulin antibody (Sigma, 1:1000) were each used at the indicated dilutions. The Mbp antibody has been described previously [46].

Neomycin Treatment

Beginning at 36 hpf, manually dechorionated embryos were immersed in embryo medium containing appropriate concentrations of neomycin sulfate (Sigma). Solutions were changed twice daily, with approximately 12 hr between changes, until 5 dpf. Hair cell death was confirmed at 5 dpf in a subset of neomycin-treated embryos by DASPEI staining as previously described [33].

Supplemental Data

Supplemental Data include five figures and Supplemental Experimental Procedures and can be found with this article online at http://www.current-biology.com/cgi/content/full/16/7/636/DC1/.

Acknowledgments

We thank Alex Schier, Matt Rasband, and members of our lab for helpful discussions and comments on the manuscript. In addition, we thank Jim Trimmer and Matt Rasband for kindly supplying antibodies. This work was supported by grants from NIH/NINDS (NS050223, W.S.T.), the NMSS (W.S.T.), and the Rita Allen Foundation (W.S.T.), a predoctoral fellowship from the Howard Hughes Medical Institute (I.G.W.), and a postdoctoral fellowship from Deutsche Forschungsgemeinschaft (P807/1-1, H.-M.P.).

Received: November 30, 2005
Revised: February 27, 2006
Accepted: February 28, 2006
Published: April 3, 2006

References

1. Salzer, J.L. (2003). Polarized domains of myelinated axons. Neuron *40*, 297–318.
2. Barres, B.A., and Raff, M.C. (1999). Axonal control of oligodendrocyte development. J. Cell Biol. *147*, 1123–1128.
3. Jessen, K.R., and Mirsky, R. (2002). Signals that determine Schwann cell identity. J. Anat. *200*, 367–376.
4. Fields, R.D. (2004). Volume transmission in activity-dependent regulation of myelinating glia. Neurochem. Int. *45*, 503–509.
5. Kaplan, M.R., Cho, M.H., Ullian, E.M., Isom, L.L., Levinson, S.R., and Barres, B.A. (2001). Differential control of clustering of the sodium channels Na(v)1.2 and Na(v)1.6 at developing CNS nodes of Ranvier. Neuron *30*, 105–119.
6. Stevens, B., Tanner, S., and Fields, R.D. (1998). Control of myelination by specific patterns of neural impulses. J. Neurosci. *18*, 9303–9311.
7. Stevens, B., and Fields, R.D. (2000). Response of Schwann cells to action potentials in development. Science *287*, 2267–2271.
8. Waxman, S.G. (1997). Axon-glia interactions: building a smart nerve fiber. Curr. Biol. *7*, R406–R410.
9. Block, M.R., Glick, B.S., Wilcox, C.A., Wieland, F.T., and Rothman, J.E. (1988). Purification of an N-ethylmaleimide-sensitive protein catalyzing vesicular transport. Proc. Natl. Acad. Sci. USA *85*, 7852–7856.
10. Wilson, D.W., Wilcox, C.A., Flynn, G.C., Chen, E., Kuang, W.J., Henzel, W.J., Block, M.R., Ullrich, A., and Rothman, J.E. (1989). A fusion protein required for vesicle-mediated transport in both mammalian cells and yeast. Nature *339*, 355–359.
11. Sollner, T., Bennett, M.K., Whiteheart, S.W., Scheller, R.H., and Rothman, J.E. (1993). A protein assembly-disassembly pathway in vitro that may correspond to sequential steps of synaptic vesicle docking, activation, and fusion. Cell *75*, 409–418.
12. Pallanck, L., Ordway, R.W., and Ganetzky, B. (1995). A *Drosophila* NSF mutant. Nature *376*, 25.
13. Schiavo, G., Gmachl, M.J., Stenbeck, G., Sollner, T.H., and Rothman, J.E. (1995). A possible docking and fusion particle for synaptic transmission. Nature *378*, 733–736.
14. Kawasaki, F., Mattiuz, A.M., and Ordway, R.W. (1998). Synaptic physiology and ultrastructure in comatose mutants define an in vivo role for NSF in neurotransmitter release. J. Neurosci. *18*, 10241–10249.
15. Tolar, L.A., and Pallanck, L. (1998). NSF function in neurotransmitter release involves rearrangement of the SNARE complex downstream of synaptic vesicle docking. J. Neurosci. *18*, 10250–10256.
16. Whiteheart, S.W., Schraw, T., and Matveeva, E.A. (2001). N-ethylmaleimide sensitive factor (NSF) structure and function. Int. Rev. Cytol. *207*, 71–112.
17. Brosamle, C., and Halpern, M.E. (2002). Characterization of myelination in the developing zebrafish. Glia *39*, 47–57.
18. Gilmour, D.T., Maischein, H.M., and Nusslein-Volhard, C. (2002). Migration and function of a glial subtype in the vertebrate peripheral nervous system. Neuron *34*, 577–588.
19. Rasband, M.N., Peles, E., Trimmer, J.S., Levinson, S.R., Lux, S.E., and Shrager, P. (1999). Dependence of nodal sodium channel clustering on paranodal axoglial contact in the developing CNS. J. Neurosci. *19*, 7516–7528.
20. Hortsch, M. (2000). Structural and functional evolution of the L1 family: are four adhesion molecules better than one? Mol. Cell. Neurosci. *15*, 1–10.
21. Neuhauss, S.C., Biehlmaier, O., Seeliger, M.W., Das, T., Kohler, K., Harris, W.A., and Baier, H. (1999). Genetic disorders of vision revealed by a behavioral screen of 400 essential loci in zebrafish. J. Neurosci. *19*, 8603–8615.
22. Vale, R.D. (2000). AAA proteins. Lords of the ring. J. Cell Biol. *150*, F13–F19.
23. Tagaya, M., Wilson, D.W., Brunner, M., Arango, N., and Rothman, J.E. (1993). Domain structure of an N-ethylmaleimide-sensitive fusion protein involved in vesicular transport. J. Biol. Chem. *268*, 2662–2666.
24. Nagiec, E.E., Bernstein, A., and Whiteheart, S.W. (1995). Each domain of the N-ethylmaleimide-sensitive fusion protein contributes to its transport activity. J. Biol. Chem. *270*, 29182–29188.
25. Lenzen, C.U., Steinmann, D., Whiteheart, S.W., and Weis, W.I. (1998). Crystal structure of the hexamerization domain of N-ethylmaleimide-sensitive fusion protein. Cell *94*, 525–536.
26. Yu, R.C., Hanson, P.I., Jahn, R., and Brunger, A.T. (1998). Structure of the ATP-dependent oligomerization domain of N-ethylmaleimide sensitive factor complexed with ATP. Nat. Struct. Biol. *5*, 803–811.
27. Puschel, A.W., O'Connor, V., and Betz, H. (1994). The N-ethylmaleimide-sensitive fusion protein (NSF) is preferentially expressed in the nervous system. FEBS Lett. *347*, 55–58.
28. Taylor, C.M., Marta, C.B., Claycomb, R.J., Han, D.K., Rasband, M.N., Coetzee, T., and Pfeiffer, S.E. (2004). Proteomic mapping provides powerful insights into functional myelin biology. Proc. Natl. Acad. Sci. USA *101*, 4643–4648.
29. Stuermer, C.A., Rohrer, B., and Munz, H. (1990). Development of the retinotectal projection in zebrafish embryos under TTX-induced neural-impulse blockade. J. Neurosci. *10*, 3615–3626.
30. Kaethner, R.J., and Stuermer, C.A. (1994). Growth behavior of retinotectal axons in live zebrafish embryos under TTX-induced neural impulse blockade. J. Neurobiol. *25*, 781–796.
31. Gnuegge, L., Schmid, S., and Neuhauss, S.C. (2001). Analysis of the activity-deprived zebrafish mutant macho reveals an essential requirement of neuronal activity for the development of a fine-grained visuotopic map. J. Neurosci. *21*, 3542–3548.

32. Kroese, A.B., Das, A., and Hudspeth, A.J. (1989). Blockage of the transduction channels of hair cells in the bullfrog's sacculus by aminoglycoside antibiotics. Hear. Res. *37*, 203–217.
33. Harris, J.A., Cheng, A.G., Cunningham, L.L., MacDonald, G., Raible, D.W., and Rubel, E.W. (2003). Neomycin-induced hair cell death and rapid regeneration in the lateral line of zebrafish (*Danio rerio*). J. Assoc. Res. Otolaryngol. *4*, 219–234.
34. Schiavo, G., Benfenati, F., Poulain, B., Rossetto, O., Polverino de Laureto, P., DasGupta, B.R., and Montecucco, C. (1992). Tetanus and botulinum-B neurotoxins block neurotransmitter release by proteolytic cleavage of synaptobrevin. Nature *359*, 832–835.
35. Saint-Amant, L., and Drapeau, P. (2001). Synchronization of an embryonic network of identified spinal interneurons solely by electrical coupling. Neuron *31*, 1035–1046.
36. Morgan, A., and Burgoyne, R.D. (1995). Is NSF a fusion protein? Trends Cell Biol. *5*, 335–339.
37. Ordway, R.W., Pallanck, L., and Ganetzky, B. (1994). Neurally expressed *Drosophila* genes encoding homologs of the NSF and SNAP secretory proteins. Proc. Natl. Acad. Sci. USA *91*, 5715–5719.
38. Pallanck, L., Ordway, R.W., Ramaswami, M., Chi, W.Y., Krishnan, K.S., and Ganetzky, B. (1995). Distinct roles for N-ethylmaleimide-sensitive fusion protein (NSF) suggested by the identification of a second *Drosophila* NSF homolog. J. Biol. Chem. *270*, 18742–18744.
39. Golby, J.A., Tolar, L.A., and Pallanck, L. (2001). Partitioning of N-ethylmaleimide-sensitive fusion (NSF) protein function in *Drosophila melanogaster*: dNSF1 is required in the nervous system, and dNSF2 is required in mesoderm. Genetics *158*, 265–278.
40. Postlethwait, J., Amores, A., Cresko, W., Singer, A., and Yan, Y.L. (2004). Subfunction partitioning, the teleost radiation and the annotation of the human genome. Trends Genet. *20*, 481–490.
41. Siddiqi, O., and Benzer, S. (1976). Neurophysiological defects in temperature-sensitive paralytic mutants of *Drosophila melanogaster*. Proc. Natl. Acad. Sci. USA *73*, 3253–3257.
42. Mochida, S., Westenbroek, R.E., Yokoyama, C.T., Zhong, H., Myers, S.J., Scheuer, T., Itoh, K., and Catterall, W.A. (2003). Requirement for the synaptic protein interaction site for reconstitution of synaptic transmission by P/Q-type calcium channels. Proc. Natl. Acad. Sci. USA *100*, 2819–2824.
43. Kimmel, C.B., Ballard, W.W., Kimmel, S.R., Ullmann, B., and Schilling, T.F. (1995). Stages of embryonic development of the zebrafish. Dev. Dyn. *203*, 253–310.
44. Postlethwait, J.H., and Talbot, W.S. (1997). Zebrafish genomics: from mutants to genes. Trends Genet. *13*, 183–190.
45. Woods, I.G., and Talbot, W.S. (2005). The *you* gene encodes an EGF-CUB protein essential for Hedgehog signaling in zebrafish. PLoS Biol. *3*, e66. 10.1371/journal.pbio.0030066.
46. Lyons, D.A., Pogoda, H.-M., Voas, M.G., Woods, I.G., Diamond, B., Nix, R., Arana, A., Jacobs, J., and Talbot, W.S. (2005). erbb3 and erbb2 are essential for schwann cell migration and myelination in zebrafish. Curr. Biol. *15*, 513–524.